





## Article

# Determination of Kinetic and Thermodynamic Parameters of Pyrolysis of Coal and Sugarcane Bagasse Blends Pretreated by Ionic Liquid: A Step towards Optimization of Energy Systems

Saad Saeed <sup>1</sup>, Mahmood Saleem <sup>2</sup>, Abdullah Durrani <sup>2</sup>, Junaid Haider <sup>3</sup>, Muzaffar Riaz <sup>1</sup>, Sana Saeed <sup>1</sup>, Muhammad Abdul Qyum <sup>4,\*</sup>, Abdul-Sattar Nizami <sup>5</sup>, Mohammad Rehan <sup>6</sup> and Moonyong Lee <sup>4,\*</sup>

<sup>1</sup> Department of Chemical Engineering, NFC Institute of Engineering & Technology, Multan 60000, Pakistan; saadsaeed@nfciet.edu.pk (S.S.); muzaffarriaz@nfciet.edu.pk (M.R.); sanasaheed@nfciet.edu.pk (S.S.)

<sup>2</sup> Institute of Chemical Engineering & Technology, University of the Punjab, Lahore 54000, Pakistan; msaleem.icet@pu.edu.pk (M.S.); akdurani.icet@pu.edu.pk (A.D.)

<sup>3</sup> School of Energy and Chemical Engineering, Ulsan National Institute of Science and Technology, 50 UNIST-gil, Eonyang-eup, Ulju-gun, Ulsan 44919, Korea; haiderjunaid92@gmail.com

<sup>4</sup> School of Chemical Engineering, Yeungnam University, Gyeongsan 38541, Korea

<sup>5</sup> Sustainable Development Study Center, Government College University, Lahore 54000, Pakistan; asnizami@gcu.edu.pk

<sup>6</sup> Center of Excellence in Environmental Studies (CEES), King Abdulaziz University, Jeddah 21577, Saudi Arabia; dr.mohammad\_rehan@yahoo.co.uk

\* Correspondence: maqyum@yu.ac.kr (M.A.Q.); mynlee@yu.ac.kr (M.L.)



**Citation:** Saeed, S.; Saleem, M.; Durrani, A.; Haider, J.; Riaz, M.; Saeed, S.; Qyum, M.A.; Nizami, A.-S.; Rehan, M.; Lee, M. Determination of Kinetic and Thermodynamic Parameters of Pyrolysis of Coal and Sugarcane Bagasse Blends Pretreated by Ionic Liquid: A Step towards Optimization of Energy Systems. *Energies* **2021**, *14*, 2544. <https://doi.org/10.3390/en14092544>

Academic Editors: Idiano D'Adamo and Attilio Conventi

Received: 24 March 2021

Accepted: 25 April 2021

Published: 29 April 2021

**Publisher's Note:** MDPI stays neutral with regard to jurisdictional claims in published maps and institutional affiliations.



**Copyright:** © 2021 by the authors. Licensee MDPI, Basel, Switzerland. This article is an open access article distributed under the terms and conditions of the Creative Commons Attribution (CC BY) license (<https://creativecommons.org/licenses/by/4.0/>).

**Abstract:** Pyrolysis behavior of ionic liquid (IL) pretreated coal and sugarcane bagasse (SCB) blends through thermogravimetric analysis (TGA) was studied. Three blends of coal and SCB having 3:1, 1:1, and 1:3 ratios by weight were treated with 1-ethyl-3-methylimidazolium chloride ([Emim][Cl]) at 150 °C for 3 h. Untreated and IL treated blends were then analyzed under pyrolytic conditions in a TGA at a constant ramp rate of 20 °C/min. Kinetic and thermodynamic parameters were evaluated using ten Coats-Redfern (CR) models to assess reaction mechanism. Results showed that the untreated blends followed a definite pattern and were proportional to the concentration of SCB in the blends. IL treated blends exhibited a higher average rate of degradation and total weight loss, indicating that IL had disrupted the cross-linking structure of coal and lignocellulosic structure of SCB. This will enhance the energy generation potential of biomass through thermochemical conversion processes. The lower activation energy ( $E_a$ ) was calculated for IL treated blends, revealing facile thermal decomposition after IL treatment. Thermodynamic parameters, enthalpy change ( $\Delta H$ ), Gibbs free energy change ( $\Delta G$ ), and entropy change ( $\Delta S$ ), revealed that the pyrolysis reactions were endothermic. This study would help in designing optimized thermochemical conversion systems for energy generation.

**Keywords:** sugarcane bagasse; ionic liquids; pretreatment; thermogravimetric analysis; co-pyrolysis; kinetic analysis

## 1. Introduction

Climate change and global warming strongly impact the worldwide energy policy, and this trend will continue for the foreseeable future [1]. The circular economy is catching the interest of policymakers at a rapid pace to target sustainable development goals. Presently, the circular economy is only 9% of the world's economy. However, this figure is likely to change dramatically in the next 10–15 years due to numerous global commitments. There is a need to develop rapid policy decisions such as providing guidelines for specific sectors, promoting circular economy culture, mapping related jobs and skills, facilitating collaborating with industries and research centers, and fostering capacity building to accelerate circular economy.

Contrary to the linear economy, the circular economy aims to focus on the materials which can be reused to eliminate the waste disposal step as much as possible. As a result, fossil fuels such as oil, gas, and coal struggle to survive as energy resources. Moreover, for a developing country like Pakistan, reliance on imported oil for electricity generation is unsustainable. Bioenergy is one of the main contributors to the circular economy as it can lead to cheaper electricity, heat, and chemical generation. Pakistan is one of the top sugar producers in the world. Therefore, sugarcane bagasse (SCB), residual waste of processed sugarcane, can be an extremely viable bioenergy source [2].

Coal is mostly present in low-grade form, known as lignite. Despite high volatile matter, lignite suffers from hydrogen-bonded cross-linking macrostructures, which strongly hinder thermochemical conversion processes such as pyrolysis, combustion, and gasification [3]. The cross-linking reaction during thermal decomposition results in producing useless waste products, thereby lowering the process efficiency. Therefore, it is necessary to break these hydrogen bonds before subjecting lignite to thermochemical conversion.

Lignocellulosic biomass primarily consists of cellulose (40–60%), hemicelluloses (20–35%), and lignin (15–20%) [4]. Cellulose is a crystalline polymer made up of strong intermolecular as well as intramolecular forces of attraction. The complex cross-linkages make it difficult to convert lignocellulosic biomass into useful products. Therefore, efficient thermal degradation of lignocellulosic biomass requires the dissolution of the holocellulosic content to facilitating heat penetration [5].

Before thermal decomposition, pretreatment of fuel can reduce plant operation costs, mitigate global warming emissions, and increase reactivity [6]. Several pretreatment methods have been proposed to increase the thermal decomposition potential of coal and lignocellulosic biomass. Acidic and basic pretreatment methods were employed in the past as pretreatment agents [7]. Although achieving high solubility, being environmentally detrimental has forced researchers to look for more suitable alternatives. In this context, ionic liquids (ILs) are gaining recognition.

Ionic liquids (ILs) have rapidly emerged in the last decade as low vapor pressure, non-flammable, easily tailorable, recyclable, and thermally stable green pretreatment solvents [8,9]. ILs have shown promising pretreatment results for both coal and biomass for thermochemical conversion. Cummings et al. found that pretreatment of lignite by 1-butyl-3-methylimidazolium chloride [Bmim][Cl] reduced the particle size from 150–200  $\mu\text{m}$  to 10  $\mu\text{m}$  [10]. Besides, Yoon et al. showed that pretreatment of lignite by [Bmim][Cl] can increase pore size from 23.6 to 51.8 nm [11]. The research also revealed that IL pretreatment results in a more efficient fuel as  $\text{H}_2$  production during gasification was 1.63 times higher than that for untreated lignite. A study revealed that [Bmim][Cl] can dissolve 80% lignite owing to its ability to break hydrogen bonds [12]. Yu et al. found that pretreatment of sub-bituminous coal by 1-ethyl-3-methylimidazolium acetate [Emim][Ac] can significantly increase the tar yield in the pyrolysis products by 27–36% [13]. Likewise, IL pretreatment of regenerated cellulose rich material by [Emim][Ac] resulted in higher furan and phenol-rich pyrolysis oil production due to the breakage of ether bonds [14]. Studies on thermal degradation of sugarcane bagasse using different ILs revealed that the nature of cations strongly influences the pretreatment behavior, with imidazolium-based ILs facilitating thermal decomposition while phosphonium-based IL increases thermal stability. Two major factors impeding the use of ILs in many applications are economic feasibility and biodegradability. As more applications of ILs in diverse fields are discovered, the cost will come down making them more accessible. One positive aspect is the tremendous regeneration ability of ILs as pretreatment agents for thermochemical conversion processes [15].

The exigency of lowering greenhouse gas emissions forces the designers to come up with amicable solutions for coal-fired power plants [16]. One such solution is the co-processing of coal and biomass blends in power plants, as biomass is a high value renewable energy source and can considerably offset the harmful effects of coal combustion [17]. In this context, investigating the effect of IL pretreatment of coal and biomass blends is

an interesting and novel idea since the studies on IL pretreatment of such blends are extremely limited.

In this work, IL pretreatment of blends composed of low-grade coal and SCB has been investigated through thermogravimetric analysis. The IL used in this study is 1-ethyl-3-methylimidazolium chloride. Thermal decomposition characteristics of untreated and IL treated blends are compared using average rate of decomposition and peak temperature obtained from TGA data. Ten Coats-Redfern reaction models based on various reaction mechanisms have been applied to determine the kinetic and thermodynamic parameters.

## 2. Materials and Methods

### 2.1. Blending and Homogenization

Pakistani low-grade coal obtained from the Balochistan province (Duki) was selected for this study. SCB (density = 100 Kg/m<sup>3</sup>, calorific value = 17.28 MJ/Kg) was collected from Layyah sugar mill located in the southern part of Punjab province. The chemical composition of SCB was as follows: cellulose = 30.82 ± 0.11, hemicelluloses = 57.89 ± 2.19, lignin = 11.29 ± 2.29. Fritsch<sup>®</sup> mortar grinder purchased from Fritsch<sup>®</sup> international was employed to crush and ground coal particles. Fritsch<sup>®</sup> vibratory sieve shaker was used for sieving to obtain a desired average particle size of 275 µm. Shredded and dried SCB was crushed using Robot Coupe<sup>®</sup> blixer 3 followed by sieving through Fritsch<sup>®</sup> vibratory sieve shaker to obtain an average particle size of 275 µm. Homogenized blends of coal and SCB were prepared in ratios 3:1, 1:1, and 1:3, respectively. The blends were dried in an oven at 80 °C for 12 h and placed in a desiccator under inert environment. A portion of the blends was kept for characterization and thermal analysis without IL pretreatment.

### 2.2. Ionic Liquid Pretreatment

[Emim][Cl] (purity > 97% (HPLC), molecular weight = 146 g/mol, density = 1.11 g/cm<sup>3</sup>, formula = C<sub>6</sub>H<sub>11</sub>ClN<sub>2</sub>) was purchased from TCI<sup>®</sup> chemicals. Before use, IL was dried in a vacuum oven at 100 °C for 48 h. [Emim][Cl] and blends were taken in equal weights and placed in a jar fitted with a magnetic stirrer. The mixture was placed on a water bath assembly to be heated at 150 °C for 3 h. Pretreatment temperature was chosen based on earlier studies [18]. It was shown previously that a single wash is not enough to remove all the adsorbed IL from coal and requires several washes [19]. Therefore, after pretreatment, the IL pretreated blends were washed several times with distilled water to ensure that [Emim][Cl] has been removed completely. For this purpose, conductivity measurements of washed water were taken till constant reading was obtained. A hydrophilic MF<sup>®</sup> Millipore membrane filter (pore size = 0.45 µm, thickness = 150 µm) purchased from Merck<sup>®</sup> was utilized for filtration. Two layers were obtained, filter cake comprising of IL pretreated blends attached with water and filtrate containing IL and water. The recovery of IL was accomplished easily by evaporation since [Emim][Cl] is a low volatile chemical, while filter cake was dried in vacuum at 80 °C for 12 h. The untreated and IL treated blends will be mentioned as C<sub>75</sub>B<sub>25</sub>, C<sub>50</sub>B<sub>50</sub>, C<sub>25</sub>B<sub>75</sub>, C<sub>75</sub>B<sub>25</sub> + [Emim][Cl], C<sub>50</sub>B<sub>50</sub> + [Emim][Cl], and C<sub>25</sub>B<sub>75</sub> + [Emim][Cl] henceforth.

Macro LECO TGA 701 was employed to carry out the proximate analysis of untreated and IL treated blends using ASTM D 7582-15 standard method. Calorific values were determined using LECO bomb calorimeter using ASTM D 2015-96 standard method.

### 2.3. Thermogravimetric Analysis

The samples' thermal decomposition was investigated under pyrolytic conditions in LECO TGA 701 capable of performing thermal analysis at ramp rates ranging between 1–50 °C/min. The ramp rate in this study was kept constant at 20 °C/min for each sample. A customized program was installed in TGA, which comprised of first heating the samples from 25 °C to 105 °C and then keeping the temperature constant for 10 min to ascertain complete moisture removal. Then, the temperature was increased to 850 °C at a constant ramp rate of 20 °C/min. Isothermal conditions were maintained until the weights did not

show significant deviation in three consecutive readings. The experiments were replicated twice and considered accurate within the tolerance level of  $\pm 5\%$ .

#### 2.4. Kinetic Analysis

Several methods are available in the literature to obtain the kinetic parameters,  $E_a$  and  $A$ , categorized into model-free and model-fitting methods [20,21]. Model-free methods such as Flynn-Wall-Ozawa (FWO), Kissinger-Akahira-Sunose (KAS), and Friedman methods are accurate but do not give information about the reaction mechanism. On the other hand, model-fitting methods give a better understanding of reaction mechanisms with less experimental data. In this study, four reaction mechanisms were tested using ten Coats-Redfern integral solution models.

The following equation generally represents heterogeneous solid-state reactions:

$$\frac{d\alpha}{dT} = \frac{1}{\beta} \cdot k(T) \cdot f(\alpha), \quad (1)$$

where  $\alpha$  is the extent of conversion,  $f(\alpha)$  is the reaction mechanism function,  $\beta$  is the ramp rate, and  $k(T)$  is the rate constant as a function of temperature. Extent of conversion can be calculated as follows:

$$\alpha = \frac{w_0 - w_t}{w_0 - w_f} \quad (2)$$

where  $w_0$ ,  $w_t$ , and  $w_f$  are the initial, instantaneous, and final weights of the sample. Replacing  $k(T)$  by using Arrhenius law gives:

$$\frac{d\alpha}{dT} = \frac{A}{\beta} e^{-E_a/RT} \cdot f(\alpha), \quad (3)$$

$A$  depends on the number of effective collisions between the reactant molecules. Integrating Equation (3) gives:

$$g(\alpha) = \frac{A}{\beta} \int_{T_0}^T \exp\left[-\frac{E_a}{RT}\right] dT, \quad (4)$$

where  $T_0$  and  $T$  are the initial and final pyrolysis temperatures, respectively. Integral solution of Equation (4) given by Coats-Redfern is as follows:

$$\ln\left[\frac{g(\alpha)}{T^2}\right] = \ln\frac{AR}{\beta E_a} \left[1 - \frac{2RT}{E_a}\right] - \frac{E_a}{RT}, \quad (5)$$

$E_a$  and  $A$  can be obtained by considering Equation (5) as equation of straight line. Ten models: first order (N1); one and a half order (N1.5); second order (N2); third order (N3); power law (PL); Mampel power law (MPL); Avrami-Erofeev equations (AE1.5 and AE2); parabolic law (D1); and Valensi equation (D2) were used in this study. These models are connected to various mechanisms by which the thermal decomposition of samples is assumed to take place.  $f(\alpha)$  and  $g(\alpha)$  associated with these models are described in Table 1.

**Table 1.** Description of CR models for estimation of kinetic and thermodynamic parameters.

Symbol	Reaction Mechanism	f(α)	g(α)
N1	Chemical reaction orders	1 − α	−ln(1 − α)
N1.5		$[(1 - \alpha)]^{3/2}$	$2[(1 - \alpha)^{-1/2} - 1]$
N2		$[(1 - \alpha)]^2$	$(1 - \alpha)^{-1} - 1$
N3		$[(1 - \alpha)]^3$	$\frac{[(1 - \alpha)^{-2} - 1]}{2}$
PL	Acceleration	1	α
MPL		$(1 - \alpha)^{1/2}$	$\alpha^{1/2}$
AE1.5	Random nucleation and subsequent growth	$3(1 - \alpha) [-\ln(1 - \alpha)]^{2/3}$	$[-\ln(1 - \alpha)]^{2/3}$
AE2		$2(1 - \alpha) [-\ln(1 - \alpha)]^{1/2}$	$[-\ln(1 - \alpha)]^{1/2}$
D1	Diffusion	1/2α	α <sup>2</sup>
D2		$[-\ln(1 - \alpha)]^{-1}$	$\alpha + (1 - \alpha) \ln(1 - \alpha)$

### 2.5. Thermodynamic Parameters

Thermodynamic parameters, ΔH, ΔG, and ΔS, can be obtained from the thermal degradation data as shown previously [22]. Following expressions were used for this purpose:

$$\Delta H = E_a - RT \quad (6)$$

$$\Delta G = E_a + RT_p \ln \left( \frac{K_B T}{hA} \right) \quad (7)$$

$$\Delta S = \frac{\Delta H - \Delta G}{T_p} \quad (8)$$

where T = mean pyrolysis temperature

$K_B$  = Stefan Boltzmann constant =  $1.381 \times 10^{-23} \text{ m}^2 \cdot \text{kg} \cdot \text{s}^{-2} \cdot \text{K}^{-1}$

h = Planck constant =  $6.626 \times 10^{-34} \text{ m}^2 \cdot \text{kg} \cdot \text{s}^{-1}$

## 3. Results

### 3.1. Proximate Analysis

Table 2 lists the proximate analysis of untreated and IL treated coal SCB blends. As evident, the properties follow a certain pattern. As the concentration of SCB increases in the blend, volatile matter (VM) increases, whilst fixed carbon (FC) and ash decreases.

**Table 2.** Proximate analysis of untreated and IL treated blends.

Samples	Proximate Analysis (wt. % on Dry Basis)			Volatility (VM/FC)	HHV (MJ/kg)
	VM	FC	Ash		
C <sub>75</sub> B <sub>25</sub>	56.36	26.79	16.85	2.10	18.20
C <sub>50</sub> B <sub>50</sub>	68.84	19.34	11.83	3.56	17.53
C <sub>25</sub> B <sub>75</sub>	79.22	13.82	6.96	5.73	17.22
C <sub>75</sub> B <sub>25</sub> + [Emim][Cl]	54.33	34.39	11.27	1.58	20.65
C <sub>50</sub> B <sub>50</sub> + [Emim][Cl]	68.63	23.97	7.40	2.86	19.18
C <sub>25</sub> B <sub>75</sub> + [Emim][Cl]	78.55	17.73	3.72	4.43	18.53

VM, FC, and ash of individual coal on dry basis were 46.61%, 32.05%, and 21.82%, respectively. In the case of SCB, VM, FC, and ash on dry basis were 91.28%, 6.88%, and 1.83%, respectively. Weighted average values correspond closely to those obtained by the experiment. IL treatment increased the HHV of the blends C<sub>75</sub>B<sub>25</sub>, C<sub>50</sub>B<sub>50</sub>, and C<sub>25</sub>B<sub>75</sub> by 13%, 9%, and 8% respectively.

### 3.2. Thermogravimetric Analysis

Figure 1 shows TG and DTG profiles of untreated and [Emim][Cl] treated blends. The profiles can be conveniently divided into three main stages: stage 1 covering temperature range 25–200 °C, stage 2 covering temperature range 200–500 °C, and stage 3 covering temperature range 500–850 °C. Stage 1 is associated with moisture removal. Stage 2 is the main devolatilization stage. Stage 3 shows lower mass loss before the curve levels off.

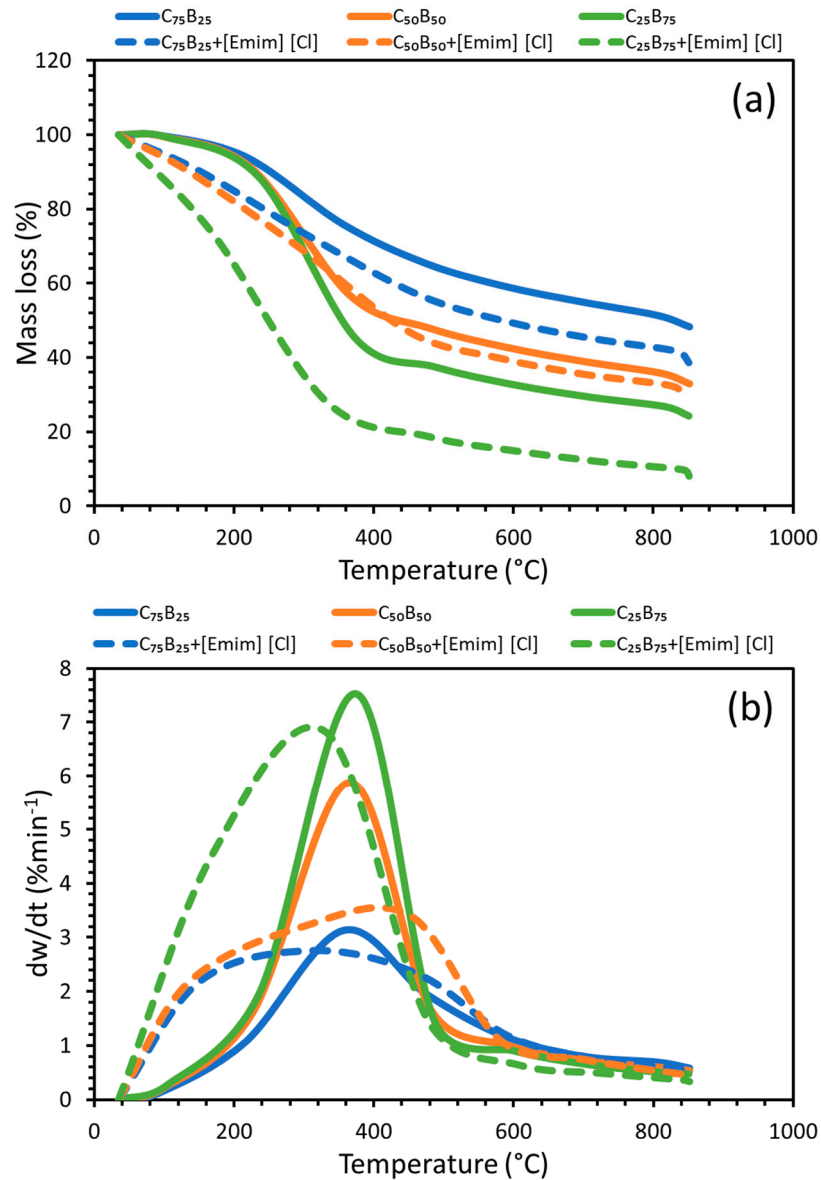


**Figure 1.** (a) TG and (b) DTG profiles of untreated and [Emim][Cl] treated coal SCB blends.

TG and DTG curves of [Emim][Cl] treated blends are also displayed in Figure 1. As the samples contained higher moisture content, rapid mass loss occurred in stage 1, represented by curves having sharp slopes. In stage 2, IL treated blends showed higher devolatilization rates as compared to untreated blends. IL treatment increased the average rate of decomposition of C<sub>75</sub>B<sub>25</sub>, C<sub>50</sub>B<sub>50</sub>, and C<sub>25</sub>B<sub>75</sub> by 22%, 7%, and 21% respectively. This signals absence of any particular trend. The temperature at which the maximum rate of decomposition takes place is called peak temperature.

### 3.3. Kinetic Analysis

Ten models based on CR integral solution model were employed to determine kinetic parameters,  $E_a$  and  $A$ .  $E_a$  and  $R^2$  values for each sample are shown in Figure 2. High  $R^2$  values were obtained for the untreated coal SCB blends. The range of  $R^2$  values for  $C_{75}B_{25}$ ,  $C_{50}B_{50}$ , and  $C_{25}B_{75}$  were 0.90–0.97, 0.90–0.97, and 0.89–0.97, respectively. The highest  $R^2$  value for all three blends was obtained for the third order reaction model (N3). However, all the models gave acceptable  $R^2$  values ranging within 0.90–0.99, except PL, MPL, D1, and D2 models for  $C_{25}B_{75} + [Emim][Cl]$  samples, which were within 0.84–0.90. Since the models giving comparatively low  $R^2$  values were for acceleration (PL and MPL) and diffusion (D1 and D2) reaction mechanisms, this implies that the decomposition reactions may not be explained well using these mechanisms. For the ten models,  $E_a$  values for  $C_{75}B_{25}$ ,  $C_{50}B_{50}$ , and  $C_{25}B_{75}$  were found to be in the ranges 12.48–51.17 kJ/mol, 12.53–46.07 kJ/mol, and 10.85–45.40 kJ/mol, respectively.

$E_a$  and  $R^2$  values for  $[Emim][Cl]$  treated coal SCB blends are displayed in parts Figure 2. Higher  $R^2$  values were obtained for IL treated blends, in the range of 0.97–0.99, 0.96–0.99, and 0.86–0.98 for the IL treated  $C_{75}B_{25}$ ,  $C_{50}B_{50}$ , and  $C_{25}B_{75}$ , respectively. It could be seen that IL treatment caused considerable reduction in the  $E_a$  values. For the ten models,  $E_a$  values for  $C_{75}B_{25} + [Emim][Cl]$ ,  $C_{50}B_{50} + [Emim][Cl]$ , and  $C_{25}B_{75} + [Emim][Cl]$  were found to be in the ranges 5.03–21.61 kJ/mol, 5.13–21.63 kJ/mol, and 3.43–31.78 kJ/mol, respectively.

### 3.4. Thermodynamic Analysis

Thermodynamic parameters,  $\Delta H$ ,  $\Delta G$ , and  $\Delta S$ , were calculated for the untreated and IL treated blends for the ten CR models. The calculated values are tabulated in Table 3. Enthalpy is a thermodynamic state function that illustrates the difference in energy level between reactants and intermediates. It also gives information about the nature of the chemical reaction. Positive  $\Delta H$  values were predicted for untreated and IL treated blends by all the models except MPL and AE2 for  $[Emim][Cl]$  treated blends. For each sample, enthalpy values were calculated using Equation 6 in which  $E_a$  values were obtained from kinetic analysis and  $T$  was the average reaction temperature. The process was applied to calculate  $\Delta H$  for the ten CR models. There was a marked difference in  $\Delta H$  values for untreated and IL treated samples, with IL treatment considerably reducing the energy required for the reaction. For example, the  $\Delta H$  value computed using N3 model for untreated  $C_{75}B_{25}$  blend was 25.32 kJ/mol whereas for IL treated blend, it was 12.48 kJ/mol. Same trend was observed with other models reporting a decrease of 10–15 kJ/mol of energy required for IL treated blends as compared to untreated blends.

The total energy released as a result of breakage of reactant bonds to form intermediates is given by  $\Delta G$ .  $\Delta G$  values for  $C_{75}B_{25}$ ,  $C_{50}B_{50}$ , and  $C_{25}B_{75}$  were in the range 128.69–143.79 kJ/mol, 126.07–141.50 kJ/mol, and 124.98–141.51 kJ/mol, respectively. Highest values were obtained for model D2 and the lowest for model N3 and the same trend was observed for the three blends.  $\Delta G$  values for IL treated  $C_{75}B_{25}$ ,  $C_{50}B_{50}$ , and  $C_{25}B_{75}$  were in the range 119.15–131.30 kJ/mol, 117.94–131.09 kJ/mol, and 109.05–128.26 kJ/mol, respectively. As with untreated blends, model D2 gave the highest and N3 the lowest values. Lower  $\Delta G$  were obtained for IL treated blends as compared to untreated blends, indicating a lower supply of energy after IL treatment. This is expected since IL treatment makes the blend easily accessible for thermal decomposition.

$\Delta S$  provides information about the thermodynamic equilibrium of a system. It is a good way to configure the structural disorder happening during a chemical reaction. Negative  $\Delta S$  were obtained for both untreated and IL treated blends, indicating higher disorder.  $\Delta S$  values for  $C_{75}B_{25}$ ,  $C_{50}B_{50}$ , and  $C_{25}B_{75}$  were in the range of  $-155.57$ – $-200.77$  kJ/mol,  $-156.72$ – $-197.61$  kJ/mol, and  $-149.40$ – $-202.12$  kJ/mol, respectively. After IL treatment,  $\Delta S$  values for  $C_{75}B_{25}$ ,  $C_{50}B_{50}$ , and  $C_{25}B_{75}$  were in the range of  $-181.40$ – $-212.29$  kJ/mol,  $-172.72$ – $-216.09$  kJ/mol, and  $-138.91$ – $-219.97$  kJ/mol, respectively.

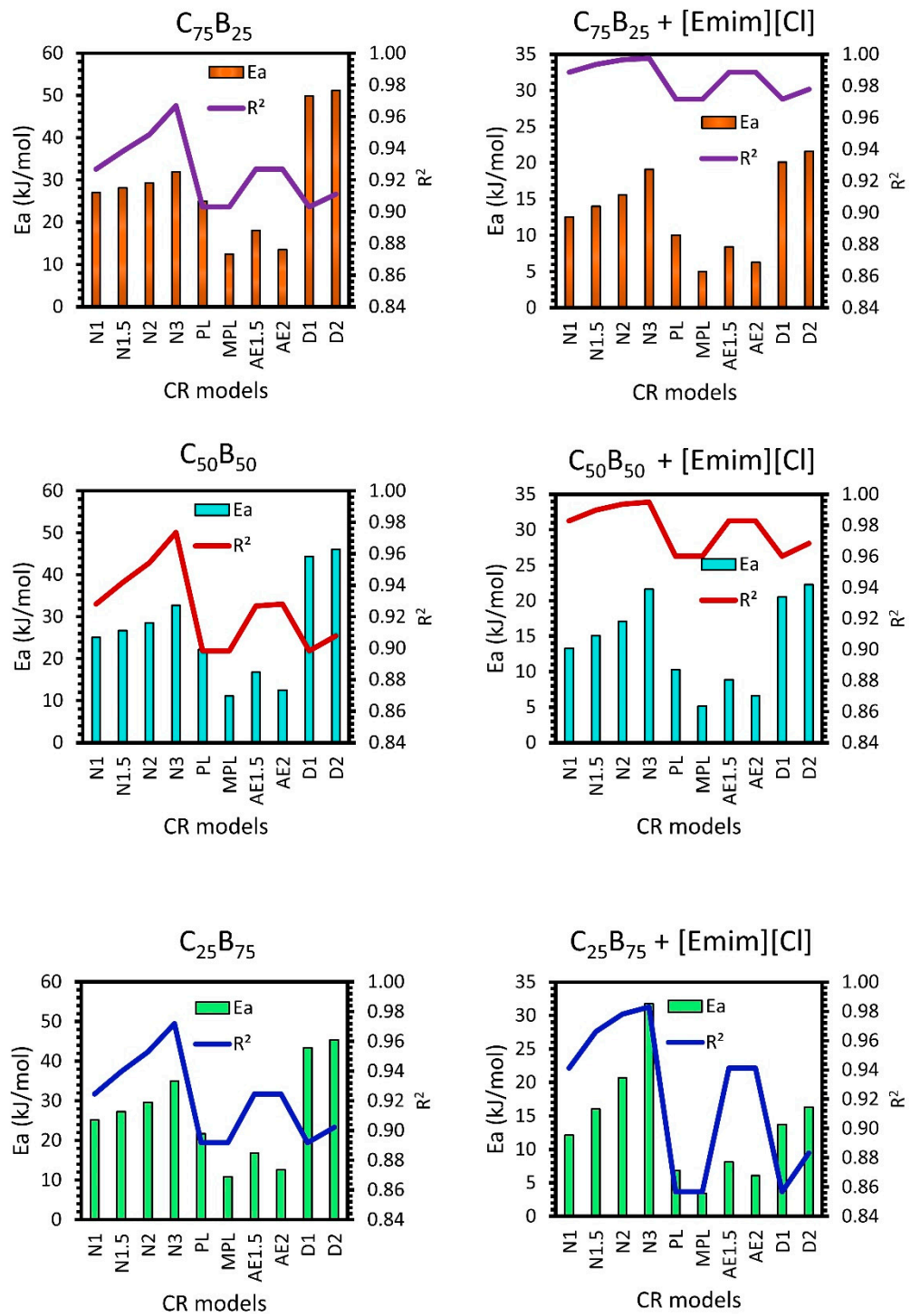


Figure 2. Ea and R<sup>2</sup> values for untreated and IL treated blends using ten CR models.



**Table 3.** Thermodynamic parameters calculated for untreated and IL treated blends.

Samples	Thermodynamic Parameters	CR Models									
		N1	N1.5	N2	N3	PL	MPL	AE1.5	AE2	D1	D2
C <sub>75</sub> B <sub>25</sub>	ΔH (kJ/mol)	20.35	21.48	22.69	25.32	18.31	5.85	11.45	6.86	43.25	44.54
	ΔG (kJ/mol)	132.22	131.40	130.53	128.69	133.73	131.93	131.09	130.96	140.95	143.79
	ΔS (J/mol. K)	−178.14	−175.03	−171.73	−164.60	−183.80	−200.77	−190.52	−197.62	−155.57	−158.05
C <sub>50</sub> B <sub>50</sub>	ΔH (kJ/mol)	18.42	20.10	21.94	26.08	15.55	4.46	10.15	5.89	37.73	39.43
	ΔG (kJ/mol)	131.77	130.46	129.07	126.07	134.09	133.45	131.60	131.97	139.05	141.50
	ΔS (J/mol. K)	−177.66	−172.99	−167.92	−156.72	−185.81	−202.19	−190.35	−197.61	−158.81	−159.98
C <sub>25</sub> B <sub>75</sub>	ΔH (kJ/mol)	18.53	20.64	22.99	28.32	15.06	4.21	10.23	5.95	36.75	38.76
	ΔG (kJ/mol)	132.30	130.65	128.87	124.98	135.17	134.99	132.55	133.15	139.26	141.51
	ΔS (J/mol. K)	−175.83	−170.03	−163.65	−149.40	−185.64	−202.12	−189.07	−196.60	−158.44	−158.80
C <sub>75</sub> B <sub>25</sub> + [Emim][Cl]	ΔH (kJ/mol)	5.92	7.36	8.95	12.48	3.42	−1.61	1.77	−0.36	13.48	14.97
	ΔG (kJ/mol)	123.75	122.63	121.49	119.15	125.91	126.09	123.95	124.47	128.94	131.30
	ΔS (J/mol. K)	−200.40	−196.03	−191.39	−181.40	−208.31	−217.17	−207.78	−212.29	−196.36	−197.84
C <sub>50</sub> B <sub>50</sub> + [Emim][Cl]	ΔH (kJ/mol)	6.64	8.44	10.44	15.00	3.63	−1.50	2.26	0.00	13.90	15.65
	ΔG (kJ/mol)	123.98	122.53	121.04	117.94	126.70	127.29	124.57	125.30	128.94	131.09
	ΔS (J/mol. K)	−196.89	−191.43	−185.56	−172.72	−206.48	−216.09	−205.22	−210.23	−193.02	−193.68
C <sub>25</sub> B <sub>75</sub> + [Emim][Cl]	ΔH (kJ/mol)	5.49	9.38	14.06	25.14	0.22	−3.21	1.49	−0.57	7.08	9.66
	ΔG (kJ/mol)	122.06	118.93	115.68	109.05	127.68	129.65	123.99	125.41	127.21	128.26
	ΔS (J/mol. K)	−192.99	−181.36	−168.24	−138.91	−211.02	−219.97	−202.80	−208.58	−198.89	−196.36

#### 4. Discussion

SCB contains higher VM and lower FC and ash as compared to lignite. Therefore, the proximate analysis results are expected and concur with the previous reports [20,21]. As the weighted average values correspond closely to those obtained by the experiment, this rules out significant synergistic effects introduced because of interplay between individual fuels in blends. Akinwale et al. [20] found that the actual VM of coal SCB blends was slightly higher than the calculated values. However, it followed a linear path.

Proximate analysis results of [Emim][Cl] treated blends showed a decrease in VM and increase in FC as well as ash. Our recent study on [Emim][Cl] pretreatment of low-rank coal revealed reduction in VM content from 46.61% to 40.23% [19]. Present results are consistent with those findings. Higher FC content points to a higher char yield during the devolatilization process. Less ash content suggests possibility of a greater mass availability for thermal decomposition. Lower ash is also beneficial for operational equipment due to less fly ash and slag formation [23]. The results also suggest that IL treatment affects the properties of coal-rich blend more than vice versa. IL treatment enhanced the HHV of the blends, which is consistent with the results obtained for individual lignite and SCB. The comparison of the results with our recent study in which blends having same composition were treated with phosphonium based IL (Trihexyltetradecylphosphonium Chloride ([P<sub>66614</sub>][Cl])) indicated contrasting results [24]. [P<sub>66614</sub>][Cl] increased VM and decreased FC appreciably while ash was also lowered, suggesting nature of cation plays a vital part in the overall behavior of IL. Another important point to consider is that [P<sub>66614</sub>][Cl], being hydrophobic, was completely absorbed in the samples, which greatly influenced its results.

As reflected in the Figure 1, thermal decomposition of untreated blends followed a definite template. Blends broke away at the start of stage 2 proportional to the amount of SCB in the blends. As content of SCB increases the amount of volatiles, higher and rapid mass loss was acquired for C<sub>25</sub>B<sub>75</sub> and C<sub>50</sub>B<sub>50</sub> blends. Average rate of decomposition for the blends C<sub>75</sub>B<sub>25</sub>, C<sub>50</sub>B<sub>50</sub>, and C<sub>25</sub>B<sub>75</sub> were 1.06 %min<sup>−1</sup>, 1.35 %min<sup>−1</sup>, and 1.52 %min<sup>−1</sup>,

respectively. In addition, blends with higher SCB content also showed a higher percentage of mass loss due to lower ash content. The total mass loss for C<sub>75</sub>B<sub>25</sub>, C<sub>50</sub>B<sub>50</sub>, and C<sub>25</sub>B<sub>75</sub> were 84.44%, 90.98%, and 94.95%, respectively. The maximum decomposition rate increased with the increase in the concentration of SCB, recording values of 3.13 %min<sup>-1</sup>, 5.88 %min<sup>-1</sup>, and 7.54 %min<sup>-1</sup> for C<sub>75</sub>B<sub>25</sub>, C<sub>50</sub>B<sub>50</sub>, and C<sub>25</sub>B<sub>75</sub>, respectively. Akinwale et al. [25] studied the TG curves of coal SCB blends for synergy and found that the slight deviation from the calculated weighted average values was observed in the temperature range 300–500 °C, indicating synergistic effects. Contrary to our results, two peaks were observed for each coal SCB blend in the temperature range 200–400 °C. The discrepancy could be attributed to coal rank, as hard South African coal has high FC and ash content compared to low-rank lignite coal used in the present study. Nonetheless, the trends observed for average and maximum thermal decomposition rates are in line with those reported previously.

IL treatment shifted the DTG curves to the left, decreasing peak temperature in the process. Peak temperatures for C<sub>75</sub>B<sub>25</sub>, C<sub>50</sub>B<sub>50</sub>, and C<sub>25</sub>B<sub>75</sub> were 356 °C, 365 °C, and 374 °C, respectively, while after IL treatment, peak temperatures reduced to 314 °C, 323 °C, and 332 °C, respectively. Comparatively, [P<sub>66614</sub>][Cl] exhibited much higher peak temperatures, which was attributed to the absorption of less volatile organic constituents of the IL by the blends. Another notable finding was the increase in the total mass loss affected by [Emim][Cl] treatment. IL treatment increased the total mass loss of C<sub>75</sub>B<sub>25</sub>, C<sub>50</sub>B<sub>50</sub>, and C<sub>25</sub>B<sub>75</sub> from 84.44%, 90.98%, and 94.95% to 91.70%, 93.75%, and 98.11%, respectively, which were close to those observed with [P<sub>66614</sub>][Cl]. Shi et al. [26] assigned temperature ranges of DTG curves to breakage of specific bonds in coal. According to the study, temperature range 300–400 °C corresponds to the cleavage of C<sub>al</sub>-O, C<sub>al</sub>-S, C<sub>al</sub>-N, and S-S bonds. Meanwhile, the temperature range 400–500 °C represents breakage of C<sub>al</sub>-C<sub>al</sub>, C<sub>al</sub>-H, C<sub>al</sub>-O, and C<sub>ar</sub>-N bonds. The DTG curves for IL treated blends showed higher. As the blends pretreated by [Emim][Cl] showed higher thermal degradation rate in the temperature range 300–500 °C, it could be assumed that IL accelerated the dissociation of the assigned bonds in this region. Besides, IL treatment has been reported to reduce the crystalline cellulose and cause disruption of the lignocellulosic structure of biomass, facilitating thermal decomposition [27]. Studies on [Emim][Ac] pretreatment of cellulose have reported the conversion of crystalline to amorphous cellulose, evidenced by the presence of two peaks in DTG curves [28]. However, our results show a single peak, which rules out the conversion of crystalline cellulose.

As regards to kinetic analysis, a wide range of values obtained for E<sub>a</sub> indicates a multiple-step reaction mechanism due to complex reactions involving the formation of activated complexes. Similar results were found for sewage sludge and rice husk blends. The Highest E<sub>a</sub> values were calculated for model N3, while the lowest for model MPL. In the case of model N3 having the highest linearity, E<sub>a</sub> values for C<sub>75</sub>B<sub>25</sub>, C<sub>50</sub>B<sub>50</sub>, and C<sub>25</sub>B<sub>75</sub> were 31.96 kJ/mol, 32.71 kJ/mol, and 34.96 kJ/mol, respectively. This suggests that the increase in the concentration of SCB increases E<sub>a</sub>. As lignocellulosic biomass has a higher thermal decomposition rate due to hemicellulose and cellulose, increase of its concentration in coal blend should presumably facilitate thermal degradation by lowering the E<sub>a</sub>. However, the results do not support this assumption. This could be explained based on synergistic interactions between coal and SCB. Such synergistic effects have also been observed in co-thermochemical conversion studies on coal and SCB [29], different coal-ranks and hazelnut shell [30]. Regarding different coal ranks, peat and lignite show greater synergy than higher rank coals. Kinetic analysis of coal SCB blends using model-free approach elucidates the relation between conversional fraction (α) and E<sub>a</sub>. One such study observed that the deviation of E<sub>a</sub> from predicted values for coal SCB blends occurred at higher α (α > 0.3).

A similar large variation in the E<sub>a</sub> values for IL treated SCB blends points to several reaction mechanisms at play during the complex breaking and formation of reactant product bonds. It is interesting to compare the E<sub>a</sub> values obtained using model N3, having

highest  $R^2$  values, for untreated and IL treated blends. On calculation, it was found that  $E_a$  values for  $C_{75}B_{25}$ ,  $C_{50}B_{50}$ , and  $C_{25}B_{75}$  after IL treatment experienced a reduction of 40.17%, 33.87%, and 9.11%, respectively, which suggests that IL treatment influenced the blends having higher coal concentration. This was also observed in proximate analysis values. In the case of  $[P_{66614}][Cl]$ ,  $E_a$  decreased by somewhat small amount. It could be implied that the cation  $[Emim]$  facilitated thermal decomposition of blends more than  $[P_{66614}]$ . In a recent study,  $[Emim][Cl]$  was able to decrease the  $E_a$  of lignite. Similar results have been obtained for  $[Bmim][Cl]$  treatment of sugarcane straw and rubberwood [31] in other studies. In the case of coal, decrease in the pore size and cleavage of cross-linked hydrogen bonding, whilst for SCB, destruction of hemicellulose and cellulose, might be the possible reasons for the significant reduction in  $E_a$  after IL treatment. As lower  $E_a$  translates into less energy consumption and ultimately less operating cost, it could be concluded that IL treatment can lower the operating cost of thermochemical conversion of coal SCB blends.

In terms of thermodynamic analysis, like  $E_a$ , a wide variation in  $\Delta H$  values was noted. For IL treated blends, much lower  $\Delta H$  values were obtained, suggesting the suppression of energy level between reactant and intermediates. Negative  $\Delta H$  values were obtained for two models, MPL and AE2, indicating exothermic reaction. However, most of the models predicted positive  $\Delta H$  values indicating endothermic reaction. This disagreement comes about because the MPL and AE2 models tend to underestimate the  $E_a$ . As seen previously, MPL and AE2 models gave low  $R^2$  values, indicating relatively poor linearity and hence, can be overlooked in favor of the models giving higher linearity. Therefore, it can be assumed that the decomposition reactions were endothermic in nature. Similar disagreement in CR models was also obtained in previous works [32]. Moreover, the difference between  $E_a$  and  $\Delta H$  provides a clue about the likelihood of pyrolysis reaction. In this study, the difference obtained was 6.63 kJ/mol. Studies have suggested that a difference of less than 5 kJ/mol means pyrolysis reaction is highly favorable [33].

The higher  $\Delta S$  values for IL treated blends show higher fragmentation of the IL treated blends than untreated ones. Higher  $\Delta S$  values were also estimated for IL pretreated oil palm biomass [34].

The results have been obtained on lab scale. There is a need to explore more ILs as potential pretreatment agents for coal and biomass blends undergoing thermochemical conversion. In this respect, software like COSMO-RS of artificial intelligence models can help narrow down the effective ILs. For efficient use of such software/models, the influential parameters of ILs defining their pretreatment capacity must be identified, which was also one of the objectives of this study. Once efficient and cost-effective ILs are specified, experiments can be performed at pilot scale and eventually, at industrial level.

## 5. Conclusions

In this work, effect of  $[Emim][Cl]$  pretreatment on the pyrolysis behavior of coal SCB blends has been investigated. Proximate analysis shows that IL lowers the volatility and ash content of the blends. Thermal analysis profiles reveal a higher average decomposition rate and total weight loss, indicating greater thermal degradation in IL treated blends. Kinetic analysis gives high  $R^2$  values for the ten CR models, suggesting multi-step reaction mechanisms for untreated and IL treated blends. Lower  $E_a$  values for IL treated blends further affirm the greater susceptibility of IL treated blends to thermal degradation. It could be concluded that  $[Emim][Cl]$  accelerates the cleavage of bonds and disruption of lignocellulosic structure in coal and SCB resulting in higher and more rapid thermal decomposition. The generated kinetic and thermodynamic data could be useful in designing large-scale systems and identifying task-specific ILs using modern software tools. In the future, a pilot-scale investigation of IL pretreated thermochemical conversion of coal biomass blends could be carried out. Since the cost of ILs is a major obstacle stopping them from realizing their true potential, regeneration could also be investigated as future research. Moreover, other biomass such as wheat straw, corncob, and rice husk etc. could be used as a replacement for SCB.

**Author Contributions:** Conceptualization, S.S. (Saad Saeed), M.S., and A.D.; methodology, S.S. (Saad Saeed); investigation, S.S. (Saad Saeed), S.S. (Sana Saeed), and M.R. (Muzaffar Riaz); resources, S.S. (Saad Saeed); data curation, M.R. (Muzaffar Riaz); writing—original draft preparation, S.S. (Saad Saeed); writing—review and editing, J.H., A.-S.N., M.R. (Mohammad Rehan), and M.A.Q.; supervision, M.S., A.D., M.L., M.A.Q. All authors have read and agreed to the published version of the manuscript.

**Funding:** This research received no external funding.

**Institutional Review Board Statement:** Not applicable.

**Informed Consent Statement:** Not applicable.

**Data Availability Statement:** Not applicable.

**Acknowledgments:** The authors would like to acknowledge Sadiq Hussain for his continuous support in the completion of this manuscript. We would also like to thank the management of “Coal Research Center” for their cooperation and support throughout this work.

**Conflicts of Interest:** The authors declare no conflict of interest.

## References

1. Al Irsyad, M.I.; Halog, A.; Nepal, R. Renewable energy projections for climate change mitigation: An analysis of uncertainty and errors. *Renew. Energy* **2019**, *130*, 536–546. [[CrossRef](#)]
2. Wu, Z.; Li, Y.; Zhang, B.; Yang, W.; Yang, B. Co-pyrolysis behavior of microalgae biomass and low-rank coal: Kinetic analysis of the main volatile products. *Bioresour. Technol.* **2019**, *271*, 202–209. [[CrossRef](#)] [[PubMed](#)]
3. Yan, J.; Jiao, H.; Li, Z.; Lei, Z.; Wang, Z.; Ren, S.; Shui, H.; Kang, S.; Yan, H.; Pan, C. Kinetic analysis and modeling of coal pyrolysis with model-free methods. *Fuel* **2019**, *241*, 382–391. [[CrossRef](#)]
4. Vergara, P.; García-Ochoa, F.; Ladero, M.; Gutiérrez, S.; Villar, J.C. Liquor re-use strategy in lignocellulosic biomass fractionation with ethanol-water mixtures. *Bioresour. Technol.* **2019**, *280*, 396–403. [[CrossRef](#)]
5. Chueter, S.; Champreda, V.; Laosiripojana, N. Evaluation of combined semi-humid chemo-mechanical pretreatment of lignocellulosic biomass in energy efficiency and waste generation. *Bioresour. Technol.* **2019**, *292*, 121966. [[CrossRef](#)] [[PubMed](#)]
6. Saeed, S.; Saleem, M.; Durrani, A. Thermal performance analysis of sugarcane bagasse pretreated by ionic liquids. *J. Mol. Liq.* **2020**, *312*, 113424. [[CrossRef](#)]
7. Monlau, F.; Barakat, A.; Steyer, J.P.; Carrere, H. Comparison of seven types of thermo-chemical pretreatments on the structural features and anaerobic digestion of sunflower stalks. *Bioresour. Technol.* **2012**, *120*, 241–247. [[CrossRef](#)]
8. Haider, J.; Saeed, S.; Qyyum, M.A.; Kazmi, B.; Ahmad, R.; Muhammad, A.; Lee, M. Simultaneous capture of acid gases from natural gas adopting ionic liquids: Challenges, recent developments, and prospects. *Renew. Sustain. Energy Rev.* **2020**, *123*, 109771. [[CrossRef](#)]
9. Kazmi, B.; Haider, J.; Qyyum, M.A.; Saeed, S.; Kazmi, M.R.; Lee, M. Heating load depreciation in the solvent-regeneration step of absorption-based acid gas removal using an ionic liquid with an imidazolium-based cation. *Int. J. Greenh. Gas Control* **2019**, *87*, 89–99. [[CrossRef](#)]
10. Cummings, J.; Kundu, S.; Tremain, P.; Moghtaderi, B.; Atkin, R.; Shah, K. V Investigations into Physico-chemical Changes in Thermal Coals during Low Temperature Ionic Liquid Treatment. *Energy Fuels* **2015**, *29*, 7080–7088. [[CrossRef](#)]
11. Yoon, S.; Deng, L.; Namkung, H.; Fan, S.; Kang, T.J.; Kim, H.T. Coal structure change by ionic liquid pretreatment for enhancement of fixed-bed gasification with steam and CO<sub>2</sub>. *Korean J. Chem. Eng.* **2018**, *35*, 445–455. [[CrossRef](#)]
12. Lei, Z.; Zhang, Y.; Wu, L.; Shui, H.; Wang, Z.; Ren, S. The dissolution of lignite in ionic liquids. *R. Soc. Chem.* **2013**, *3*, 2385–2389. [[CrossRef](#)]
13. Yu, W.; Zhu, P.; Lei, Z.; Shui, H.; Kang, S.; Wang, Z.; Ren, S.; Pan, C. Study of pyrolysis behavior of shenhua coal pretreated by ionic liquid 1-ethyl-3-methylimidazolium acetate. *Int. J. Chem. React. Eng.* **2018**, *16*. [[CrossRef](#)]
14. Halder, P.; Kundu, S.; Patel, S.; Parthasarathy, R.; Pramanik, B.; Paz-Ferreiro, J.; Shah, K. TGA-FTIR study on the slow pyrolysis of lignin and cellulose-rich fractions derived from imidazolium-based ionic liquid pre-treatment of sugarcane straw. *Energy Convers. Manag.* **2019**, *200*. [[CrossRef](#)]
15. Saeed, S.; Shafeeq, A.; Raza, W.; Ijaz, A.; Saeed, S. Effect of regenerated ionic liquid pretreatment on the thermogravimetric analysis of spent coffee ground. *Energy Sources Part A Recover. Util. Environ. Eff.* **2020**, 1–13. [[CrossRef](#)]
16. Xu, Y.; Yang, K.; Zhou, J.; Zhao, G. Coal-biomass co-firing power generation technology: Current status, challenges and policy implications. *Sustainability* **2020**, *12*. [[CrossRef](#)]
17. Gongora, A.; Villafranco, D. Sugarcane bagasse cogeneration in Belize: A review. *Renew. Sustain. Energy Rev.* **2018**, *96*, 58–63. [[CrossRef](#)]
18. Lei, Z.; Hu, Z.; Zhang, H.; Han, L.; Shui, H.; Ren, S.; Wang, Z.; Kang, S.; Pan, C. Pyrolysis of lignite following low temperature ionic liquid pretreatment. *Fuel* **2016**, *166*, 124–129. [[CrossRef](#)]

19. Cummings, J.; Shah, K.; Atkin, R.; Moghtaderi, B. Physicochemical interactions of ionic liquids with coal; The viability of ionic liquids for pre-treatments in coal liquefaction. *Fuel* **2015**, *143*, 244–252. [[CrossRef](#)]
20. Naqvi, S.R.; Hameed, Z.; Tariq, R.; Taqvi, S.A.; Ali, I.; Niazi, M.B.K.; Noor, T.; Hussain, A.; Iqbal, N.; Shahbaz, M. Synergistic effect on co-pyrolysis of rice husk and sewage sludge by thermal behavior, kinetics, thermodynamic parameters and artificial neural network. *Waste Manag.* **2019**, *85*, 131–140. [[CrossRef](#)]
21. Chong, C.T.; Mong, G.R.; Ng, J.H.; Chong, W.W.F.; Ani, F.N.; Lam, S.S.; Ong, H.C. Pyrolysis characteristics and kinetic studies of horse manure using thermogravimetric analysis. *Energy Convers. Manag.* **2019**, *180*, 1260–1267. [[CrossRef](#)]
22. Saeed, S.; Saleem, M.; Durrani, A.K. Thermal performance analysis of low-grade coal pretreated by ionic liquids possessing imidazolium, ammonium and phosphonium cations. *Fuel* **2020**, *271*, 117655. [[CrossRef](#)]
23. Zeng, T.; Mlonka-Mędrala, A.; Lenz, V.; Nelles, M. Evaluation of bottom ash slagging risk during combustion of herbaceous and woody biomass fuels in a small-scale boiler by principal component analysis. *Biomass Convers. Biorefinery* **2019**. [[CrossRef](#)]
24. Saeed, S.; Saleem, M.; Durrani, A. Thermal performance analysis and synergistic effect on co-pyrolysis of coal and sugarcane bagasse blends pretreated by trihexyltetradecylphosphonium chloride. *Fuel* **2020**, *278*, 118240. [[CrossRef](#)]
25. Aboyade, A.O.; Görgens, J.F.; Carrier, M.; Meyer, E.L.; Knoetze, J.H. Thermogravimetric study of the pyrolysis characteristics and kinetics of coal blends with corn and sugarcane residues. *Fuel Process. Technol.* **2013**, *106*, 310–320. [[CrossRef](#)]
26. Shi, L.; Liu, Q.; Guo, X.; Wu, W.; Liu, Z. Pyrolysis behavior and bonding information of coal—A TGA study. *Fuel Process. Technol.* **2013**, *108*, 125–132. [[CrossRef](#)]
27. Perez-Pimienta, J.A.; Lopez-Ortega, M.G.; Chavez-Carvayar, J.A.; Varanasi, P.; Stavila, V.; Cheng, G.; Singh, S.; Simmons, B.A. Characterization of agave bagasse as a function of ionic liquid pretreatment. *Biomass Bioenergy* **2015**, *75*, 180–188. [[CrossRef](#)]
28. Singh, S.; Varanasi, P.; Singh, P.; Adams, P.D.; Auer, M.; Simmons, B.A. Understanding the impact of ionic liquid pretreatment on cellulose and lignin via thermochemical analysis. *Biomass Bioenergy* **2013**, *54*, 276–283. [[CrossRef](#)]
29. Aboyade, A.O.; Carrier, M.; Meyer, E.L.; Knoetze, J.H.; Görgens, J.F. Model fitting kinetic analysis and characterisation of the devolatilization of coal blends with corn and sugarcane residues. *Thermochim. Acta* **2012**, *530*, 95–106. [[CrossRef](#)]
30. Haykiri-Acma, H.; Yaman, S. Interaction between biomass and different rank coals during co-pyrolysis. *Renew. Energy* **2010**, *35*, 288–292. [[CrossRef](#)]
31. Khan, A.S.; Man, Z.; Bustam, M.A.; Kait, C.F.; Ullah, Z.; Nasrullah, A.; Khan, M.I.; Gonfa, G.; Ahmad, P.; Muhammad, N. Kinetics and thermodynamic parameters of ionic liquid pretreated rubber wood biomass. *J. Mol. Liq.* **2016**, *223*, 754–762. [[CrossRef](#)]
32. Naqvi, S.R.; Tariq, R.; Hameed, Z.; Ali, I.; Naqvi, M.; Chen, W.H.; Ceylan, S.; Rashid, H.; Ahmad, J.; Taqvi, S.A.; et al. Pyrolysis of high ash sewage sludge: Kinetics and thermodynamic analysis using Coats-Redfern method. *Renew. Energy* **2019**, *131*, 854–860. [[CrossRef](#)]
33. Ahmad, M.S.; Mehmood, M.A.; Taqvi, S.T.H.; Elkamel, A.; Liu, C.G.; Xu, J.; Rahimuddin, S.A.; Gull, M. Pyrolysis, kinetics analysis, thermodynamics parameters and reaction mechanism of *Typha latifolia* to evaluate its bioenergy potential. *Bioresour. Technol.* **2017**, *245*, 491–501. [[CrossRef](#)]
34. Mahmood, H.; Moniruzzaman, M.; Iqbal, T.; Yusup, S.; Rashid, M.; Raza, A. Comparative effect of ionic liquids pretreatment on thermogravimetric kinetics of crude oil palm biomass for possible sustainable exploitation. *J. Mol. Liq.* **2019**, *282*, 88–96. [[CrossRef](#)]